

June 2022

## SOURCES OF RESONANT VORTICES IN AERO-ACOUSTICS RESONANCE FROM TANDEM FLAT PLATES

Atef El Khatib

*Engineer, Faculty of Engineering, Beirut Arab University, a.rkhatib@bau.edu.lb*

Ahmad Al Miaari

*Engineer, Faculty of Engineering, Beirut Arab University, ahmad.miaari@gmail.com*

Ali Hammoud

*Professor, Faculty of Engineering, Beirut Arab University, ahammoud@bau.edu.lb*

Follow this and additional works at: <https://digitalcommons.bau.edu.lb/stjournal>



Part of the [Aerodynamics and Fluid Mechanics Commons](#), and the [Physical Sciences and Mathematics Commons](#)

---

### Recommended Citation

El Khatib, Atef; Al Miaari, Ahmad; and Hammoud, Ali (2022) "SOURCES OF RESONANT VORTICES IN AERO-ACOUSTICS RESONANCE FROM TANDEM FLAT PLATES," *BAU Journal - Science and Technology*: Vol. 3: Iss. 2, Article 4.

DOI: <https://www.doi.org/10.54729/XBUJ5264>

Available at: <https://digitalcommons.bau.edu.lb/stjournal/vol3/iss2/4>

This Article is brought to you for free and open access by Digital Commons @ BAU. It has been accepted for inclusion in BAU Journal - Science and Technology by an authorized editor of Digital Commons @ BAU. For more information, please contact [ibtihal@bau.edu.lb](mailto:ibtihal@bau.edu.lb).

---

## SOURCES OF RESONANT VORTICES IN AERO-ACOUSTICS RESONANCE FROM TANDEM FLAT PLATES

### Abstract

Aero-acoustic resonance in flows around flat plates is a major design concern in various practical applications, especially turbomachinery and heat exchangers, due to its significant effects on fatigue rates and radiated noises intensity. Although research has been intensive on the topic, there is still a lot to be understood for effective resonance prediction and control. Resonance in tandem plate systems is characterized by a double response. This study, investigates for the first time, the flow mechanisms responsible for the generation of low-velocity and high-velocity resonances of the double resonance response. Experimental testing and numerical simulation showed that low-velocity resonance vortices are created by normal shedding in the spacing between the plates, while high-velocity resonance vortices are formed by the interaction of vortices that are naturally shed in the gap with the downstream plate. In addition, altering the gap distance between the plates changes the flow regime responsible for the generation of resonant vortices.

### Keywords

Aero-acoustic Resonance; Flow-induced Vibrations; Shear Layers Interaction; Tandem Flat Plates; Acoustic Modes Excitation

## 1. INTRODUCTION

Aero-acoustic resonance has been a topic of interest for many researchers due to its practical applications in industry such as compressors (Di Bari et al., 2004) and heat exchangers (Eisinger & Sullivan, 2007). This resonance occurs when vortex from a bluff body shed at a frequency close to one of the surrounding duct's acoustic modes. This excites the acoustic mode and generates acoustic oscillations. The resonance involves a self-sustained mechanism between acoustic oscillations and vortex shedding called the "feedback loop" in which vortex shedding is locked at a certain frequency. Details on self-sustained mechanisms can be found in (Assoum et al., 2014) and (Assoum et al., 2013). Parker (Parker, 1967) has shown that the easiest duct's acoustic mode to be excited is the  $\beta$ -mode whose frequency can be estimated using equation (1). A main concern in aero-acoustic resonance is that it generates acoustic noises that may exceed the dynamic head of the flow causing an increase in fatigue rates and threatening mechanical failure of the system. Therefore, full understanding of the phenomenon is crucial for effective prediction and control.

$$\Omega = \frac{a}{2b} \quad (1)$$

Bluff body geometry is a key parameter that affects the vortex shedding responsible for the excitation of acoustic resonance. (Parker & Welsh, 1983) identified four different flow regimes associated with flow around a single flat plate based on its chord-to-thickness  $c/t$  ratio. The flow regimes differ in the mechanism of separation, and interaction of the shear layers. (Nakamura & Hirata, 1989) added one more regime to the ones proposed by Parker et al. (1983) and showed that these regimes affect the behavior of shedding Strouhal number. (Katasonov et al., 2015) and (Semenov & Bardakhanov, 2007) have shown that the amplitude and range of resonant velocities in flat plates are affected by the geometric profile of plate's leading and trailing edges. Despite the various flow regimes that can be established in different flat plates geometries, resonant vortex shedding are always located just downstream the trailing edge (Tan et al., 2003)(Mathias et al., 1988).

In cases of tandem bluff bodies, the vortex shedding mechanism becomes more complex as the gap between the plates is an additional geometrical parameter that affects the generation of resonant vortex shedding through the interaction of shear layers with a downstream boundary. Sakamoto et al. (Sakamoto et al., 1987) experimentally studied vortex shedding from two rectangular cylinders in tandem with different gap-to-thickness ratios ( $G$ ). They observed four different flow regimes with different locations of vortex shedding. Another classification of flow regimes based on ( $G$ ) was reported by Havel et al. (Havel et al., 2001) when they studied vortex shedding from two cubic obstacles at  $Re = 22,000$ . Another flow regime classification was proposed by Blazewicz et al. (Blazewicz et al., 2007) as they experimentally studied shear layers reattachment and interaction in tandem plates based on separation bubble length and  $c/t$  ratio. However, they did not identify the vortex shedding mechanism corresponding to each flow regime. Bull et al. (Bull et al., 1997) have shown through experimental testing that the acoustic amplitude of resonance for two sharp-edge plates in tandem changes, sometimes significantly, with the change of the associated flow regime.

Aeroacoustic resonance from tandem bluff bodies is often characterized by the excitation of the lowest duct acoustic mode at two different ranges of flow velocity. This characterization is referred to as double-resonance response. (Parker et al., 1993), (Stoneman et al., 1988), and (Mohany & Ziada, 2005). For the case of tandem cylinders, Mohany and Ziada (Mohany & Ziada, 2009b) showed, through experimental analysis and numerical simulation, that lower-velocity resonance is caused by vortex shedding downstream the tandem system while higher-velocity resonance is caused by vortex shedding between the cylinders. For the case of tandem flat plates, Parker et al. (Parker et al., 1993) showed that the lower-velocity and higher-velocity aeroacoustic resonances occur at different phase angles, signifying different flow regimes associated with each resonance. El Khatib et al. (El Khatib et al., 2021) supported this finding as they showed that the two resonances occur at different ranges of reduced velocities, consequently different ranges of Strouhal number.

Based on the above discussion, the flow regimes in the double resonance response are believed to be different but they are still not well identified. The present study discusses, for the first time, experimentally and numerically, the flow mechanisms responsible for the generation of lower-velocity and higher-velocity resonances of the double resonance response in aeroacoustic resonant from flat plates in tandem with different gap-to-distance ratios, and identifies the flow regime responsible for each resonance.

## 2. EXPERIMENTAL SETUP

Two sharp-edge flat plates with  $c/t$  ratios of 18 cm/1 cm and 10 cm/ 1.5 cm were installed at the centerline of a 0.35m x 0.35 m rectangular test section of an open-loop wind tunnel with the 18/1 plate being upstream. The test section is 1.2 m long and is made of 1.5 cm thick transparent acrylic. Air flow parallel to the direction of plate' chords with freestream velocity that reaches a maximum of 60 m/s. A Pitot-static tube with a U-tube manometer were used to calibrate the flow velocity inside the duct.

The gap distance between the plates was varied to match ( $G$ ) values of 2, 4, 6 and 8 where ( $G$ ) is defined as gap distance ( $d$ ) divided by the upstream plate thickness ( $t$ ). A 25.6 KHz sampling rate, TSI hot-wire anemometer was used to measure the vortex shedding frequency at different locations in the duct, and a 25 KHz ¼ in. GRAS NI pressure field microphone sensor was flush-mounted at the lower surface of the duct to measure the temporal coordinate of the acoustic pressure. Fig.1 shows a sketch of the experimental setup. It is worth noting that the shedding frequencies reported in the experimental results throughout the script are located in the gap between the plates.

The lowest acoustic mode of the empty duct (without plates) was found experimentally by fitting a general purpose NI accelerometer, with a sampling frequency up to 5 KHz, to the duct wall to measure the mechanical vibration of the system while inducing a sounds of different frequencies using a sound generator. The lowest duct acoustic mode frequency was found to be 490 Hz that is almost equal to the value calculated using equation (1) (491.5 Hz). The experimentally excited lowest duct acoustic mode frequency with the plates fitted is 445 Hz that is a bit lower than the empty duct acoustic mode. This agrees with the results of Parker (Parker, 1967) that adding a plate to the duct decreases its acoustic mode frequency by a small value.

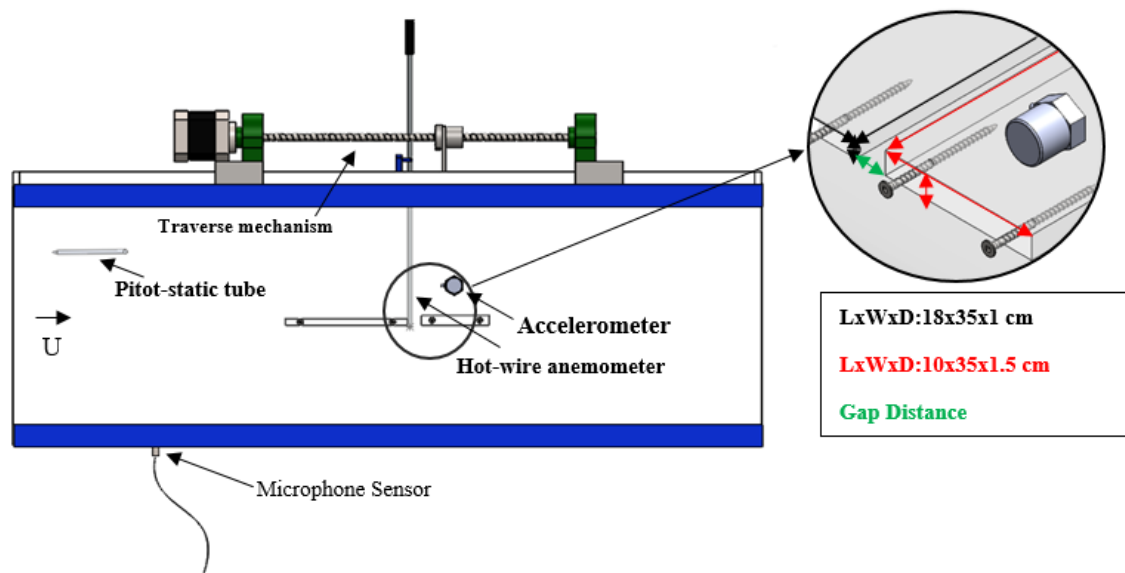


Fig.1: Sketch of the experimental setup

(Lighthill, 1952)(Belvins, 1990), and (Mohany & Ziada, 2009a) discussed that under low Mach number flows, and assuming the plates have a length that is larger than the wavelength of the acoustic radiation, and with the angle between the microphone sensor and axis of the plates being  $90^\circ$ , the sound pressure is proportional to dynamic pressure and Mach number. Therefore, the root mean square (RMS) amplitude of the sound pressure was normalized by the dynamic head and Mach number ( $M$ ) as presented in equation (2). This normalization significantly reduces the

scatter in the sound pressure as it accounts for the main parameters that affect the aero-acoustic resonance (Mohany & Ziada, 2005). Also, reduced velocity ( $U_r$ ) was used to provide generalized values of flow velocity as in equation (3).

$$P' = \frac{P_{rms}}{0.5 \rho^2 M} \quad (2)$$

$$U_r = \frac{U}{\Omega \times t} \quad (3)$$

### 3. ACOUSTIC RESPONSE OF SINGLE PLATE

Fig2 exhibits the variation of shedding frequency ( $f$ ) and the normalized acoustic pressure ( $P'$ ) with reduced velocity ( $U_r$ ) for flow over a single plate 18/1. With the increase of reduced velocity, the vortex shedding frequency increases at the natural Strouhal number ( $S_t = 0.2$ ), until it reaches a value close to the lowest acoustic mode frequency ( $\Omega$ ) at which it locks for a single range of reduced velocity, that is from 4 to 4.4 in the described case. During this lock-in state, the sound pressure increases until reaching its peak and decreasing again. Further increasing the flow velocities break the feedback loop, and the shedding frequency increases again while the resonant sound pressure decreases. This behavior matches the pattern reported in the literature of the topic (Mathias et al., 1988)(Welsh & Stokes, 1984).

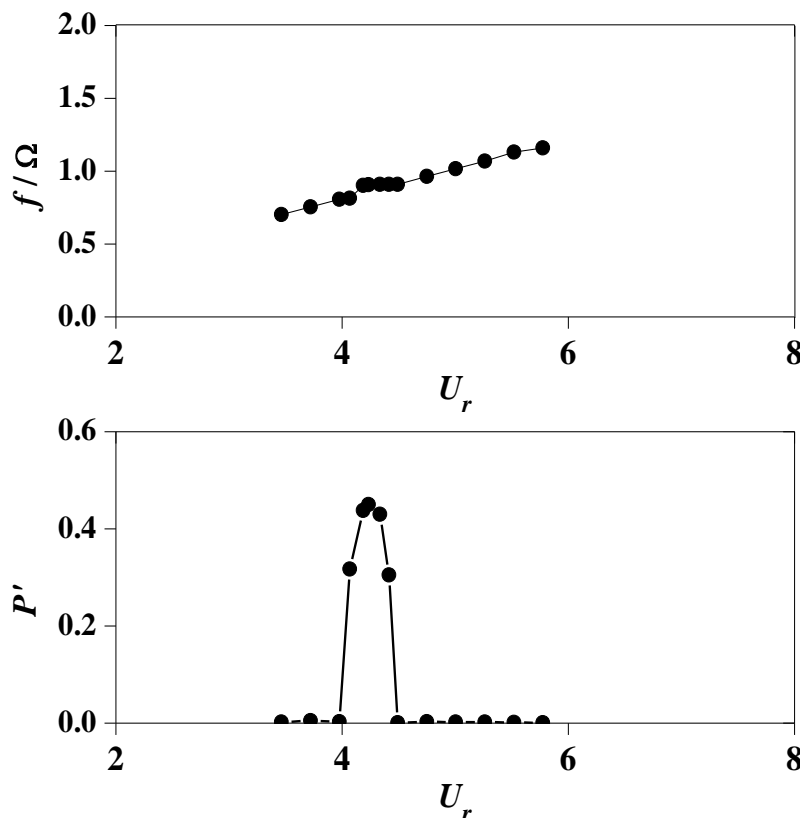


Fig2: Shedding frequency and acoustic pressure of single 18/1 plate

### 4. ACOUSTIC RESPONSE OF TWO PLATES IN TANDEM

The aero-acoustic response caused by flow over tandem flat plates, shown in Fig. 3, is similar to that of a single plate. The main difference is the presence of double resonance response in tandem system. For ( $G = 2$ ) and ( $G = 4$ ), the double resonance is continuous as the lower-velocity and higher-velocity resonances occur in the ranges of (3.7 to 4.5) and (4.7 to 7.8) in Fig. 3(a), and from (4.23 to 7.3) and (7.3 to 8.8) in Fig. 3(b). Whereas for ( $G = 6$ ) and ( $G = 8$ ) the double resonance is distinct in the ranges of (3.4 to 5), (8.08 to 9.8) and (3.4 to 5.5), (8.8 to 10.4) in Fig. 3(c) and Fig. 3(d) respectively.

In addition, two vortex shedding are present simultaneously in the gap between the plates during the higher-velocity resonance of the double response for Fig.3 (b), Fig.3 (c), and Fig.3 (d) respectively, signifying that the developed flow regime  $G = 4, 6$  and  $8$  is different than the regime established for  $G = 2$ .

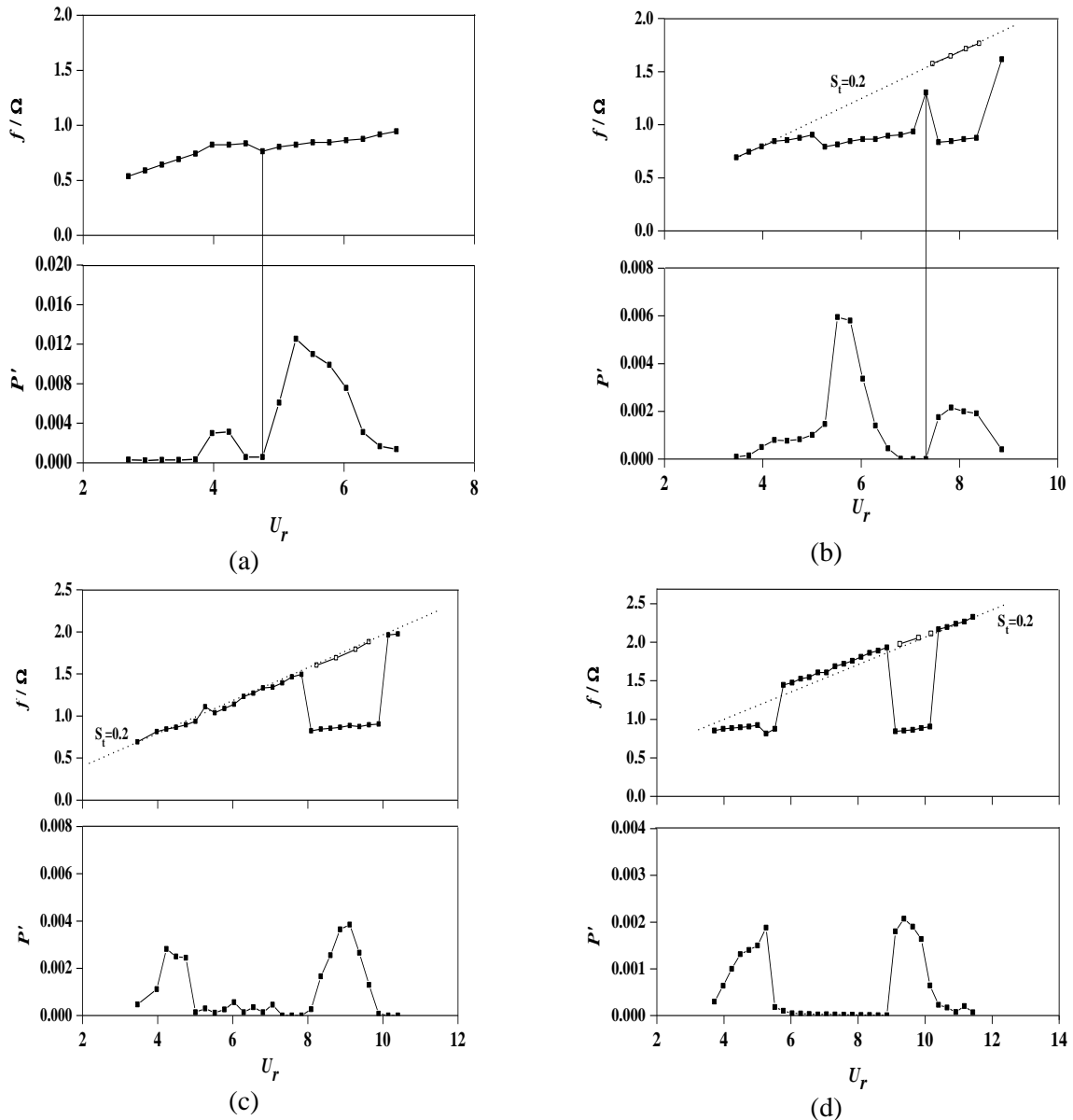


Fig3: Aero-acoustic response of tandem flat plates with (a) $G=2$  (b) $G=4$  (c) $G=6$  (d) $G=8$  (●) represents vortex shedding (○) reopresents non-resonant vortex shedding during higher-velocity resonance

In order to identify the nature of vortex shedding generated in each of the different mechanisms of lower-velocity and higher-velocity resonances, Strouhal number was calculated at the onset of each resonance, as in equation (4), and results are represented in Fig.4. Lower-velocity resonance and higher-velocity resonance are referred to as Mode 1,1 and Mode 1,2 respectively in the Fig and throughout the script.

Fore Mode1,1, results show that vortices shed at a Strouhal number value of 0.2 indicating natural vortex shedding in the gap between the plates. For Mode1,2, at  $G = 2$ , the resonant vortex shedding is non-natural as vortices shed a Strouhal number of 0.16. At  $G > 2$ , the non-resonant vortex shedding is natural, while the resonant vortices are found to be non-natural as they shed at  $S_t$  lower than 0.2. The decreasing pattern of Strouhal number in Mode1,2 shows that the resonance requires higher flow velocity to be excited with the increase of gap distance. This observation can also be noticed when comparing the reduced velocity at the onset of Mode 1,2 resonance in Fig. 3.

$$S_t = \frac{f \times t}{U} \quad (4)$$

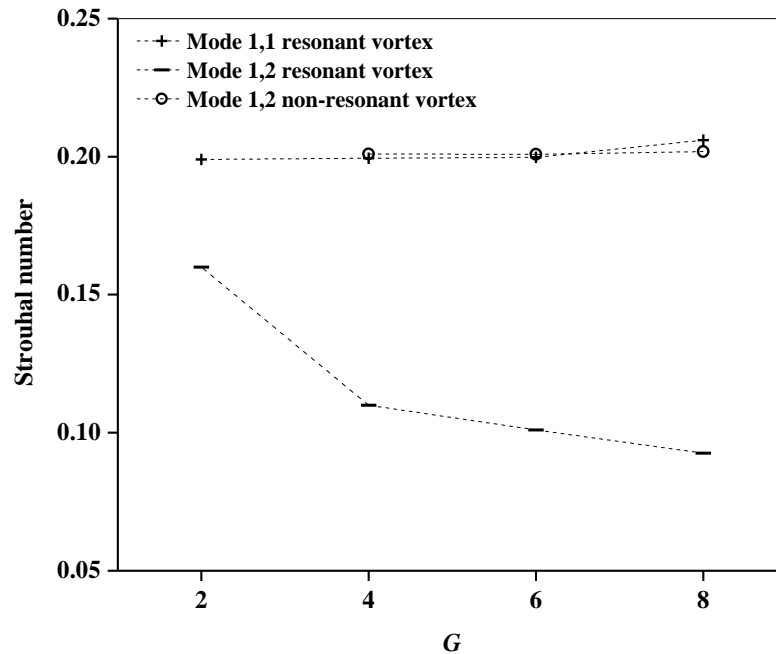


Fig.4: Strouhal number at the onset of resonance

## 5. MECHANISMS OF VORTEX GENERATION

### 5.1. Numerical Simulation

To further study the experimental results, the flow mechanism that generate the vortices in Mode1,1 and Mode1,2, a numerical simulation was performed to model the transient flow velocity at the onset of each resonance. A finite volume analysis software, ANSYS Fluent, was used with air being the working fluid. Sparat-Allmaras (Mohany & Ziada, 2009a) model was adopted for the simulation as it is developed for applications involving wall-bounded flows and it is accurate for simulating flow separation in boundary layers (Spalart & Allmaras, 1994). Unstructured triangular and quadrilateral meshes were used in a 2D plane, with grids near the plates being further refined. The number of elements is 75,200 and the grid-dependence of the solution was examined. The time step was set to  $10^{-5}$  seconds, so each vortex cycle was solved in 225 time steps.

### 5.2. Sources of Model 1,1 Vortices

Fig.5 shows a numerical simulation of streamlines at the onset of Mode1,1 resonance for all tested gap distances. For  $G = 2$ , the simulation shows vortex shedding trapped between the trailing edge and leading edge of the upstream and downstream plates respectively. This shedding is natural as previously discussed in Fig.4. For  $G > 2$ , a different flow regime is established as the separate shear layers reattach in the gap between the plates resulting in a natural resonant vortex shedding just after the upstream plate. The flow separates again at the leading edge of the downstream plate and vortices shed naturally just after the plate, but this shedding is non-resonant as it did not excite the duct's lowest acoustic mode during the experimental measurements. The simulation results agree with the experimental findings of (Parker et al., 1993)(El Khatib et al., 2021).

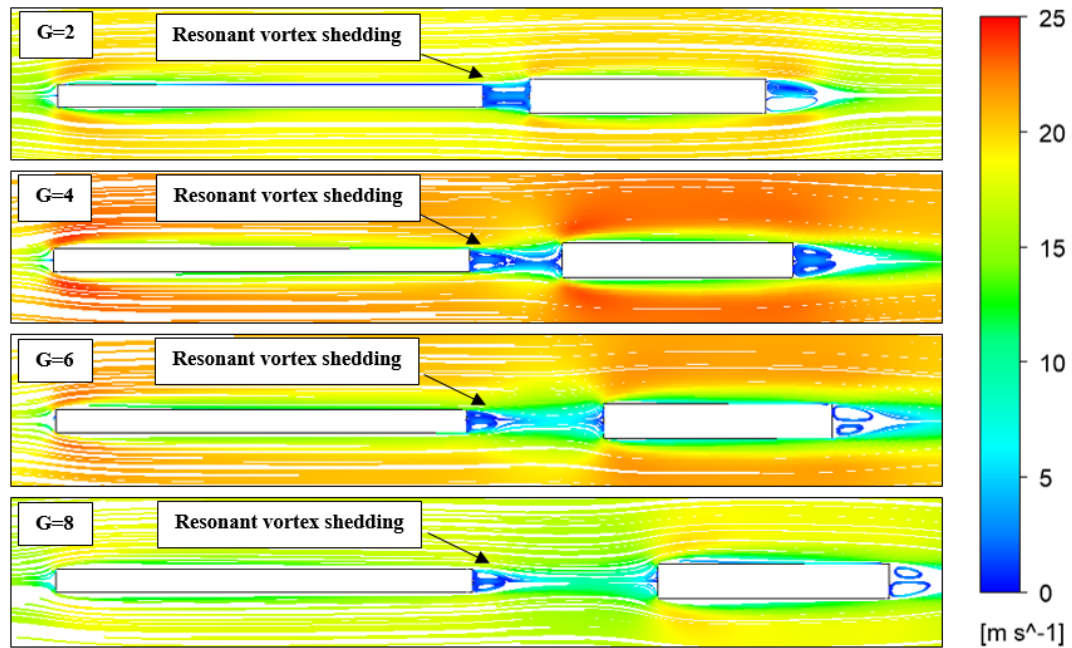


Fig.5: Simulation of streamlines at the onset of Mode1,1 resonance

### 5.3. Sources of Model 1,2 Vortices

The simulated streamlines at the onset of Mode1,2 resonance for each gap distance are presented in Fig. 6. In the case of  $G = 2$ , similar flow regime to Mode1,1 resonance is present as the vortices look trapped between the edges of the plates. However, the experimental results in Fig.4 shows that these vortices shed at a Strouhal number value different from 0.2 indicating non-natural vortex shedding. Therefore, it is suggested that at lower-velocities (Mode1,1 resonance) vortices shed naturally in the gap and get trapped between the plates. At higher flow velocity (Mode1,2 resonance) the interaction of vortices with the edges of the plates forces the shedding to be trapped in the gap. This justifies the continuous double resonance response in Fig3. Further investigation through flow visualization can verify the behavior of the trapped vortices with the increase of flow velocity.

For  $G > 2$ , simulation results in Fig. 6 are exhibited in two different instants of the flow to study the presence of two simultaneous vortex shedding observed in Fig3. The time steps are represented in terms of one cycle of vortex shedding ( $\tau$ ) that is the reciprocal of the shedding frequency ( $f$ ). The flow regime is again different from the trapped vortex established in  $G = 2$ . At  $t = \tau$ , the simulation shows natural vortex shedding just after the trailing edges of the upstream and downstream plates. These vortices are non-resonant as they did not excite any of the duct's acoustic modes during the experiments. At  $t \neq \tau$  for  $G = 4, 6$  and  $8$  respectively, the resonant vortex shedding was found almost at the leading edge of the downstream plate. The pattern of streamlines in the gap between the plates proves that these vortices are not generated from direct reattachment of shear layers at the downstream plate, but rather from the interaction of vortices that are naturally shed from the trailing edge of the upstream plate with the leading edge of the downstream plate. This justifies the presence of vortex shedding that look simultaneous during the experimental measurements as shown in Fig3.

The reason why vortices that shed from the upstream plate and interact with the downstream plate are not always resonant can be referred to the fact that the occurrence of resonance depends on the phase at which the vortices arrive corresponding to the acoustic cycle (Stokes & Welsh, 1986). This phase is affected by the convection velocity of the vortex that is dependent on the flow velocity. Therefore, a specific range of flow velocity is required for these vortices to be resonant. This justifies the presence of continuous or distinct double resonance response for different gap distances.

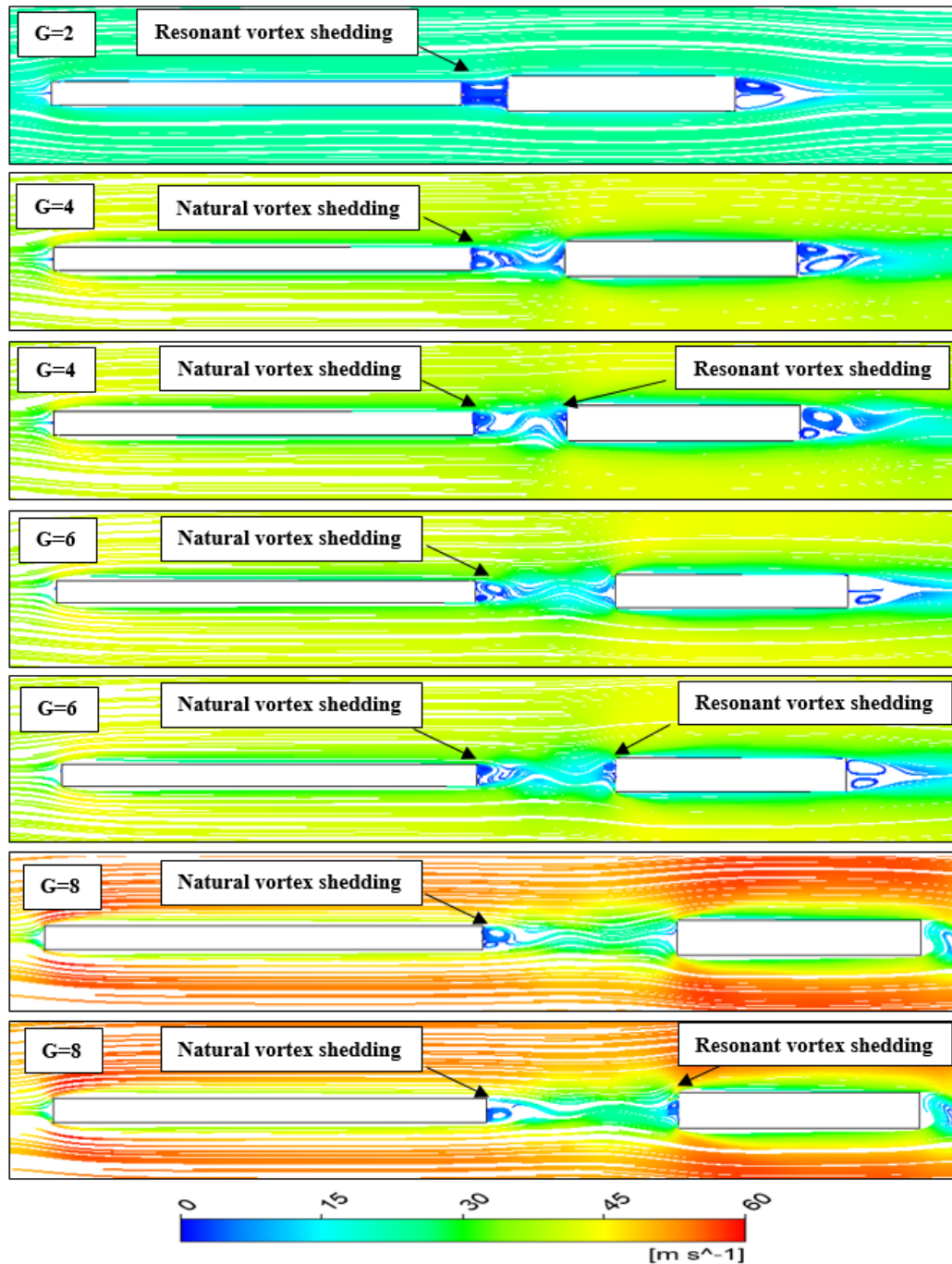


Fig.6: Simulation of streamlines at the onset of Mode 1,2 resonance

## 6. CONCLUSION

An investigation of the sources of aero-acoustic resonant vortices in flow over tandem flat plates was performed through experimental testing and numerical simulation. The following conclusions are drawn out:

1. The aero-acoustic response is characterized by a double resonance response in which lowest duct's acoustic mode is excited twice in two different ranges of flow velocities.
2. The lower-velocity resonance is caused by natural vortex shedding while the higher-velocity resonance is caused by the interaction of vortices that shed from the upstream plate with the leading edge of the downstream plate.
3. During the higher-velocity resonance, two vortices are shed in the gap between the plates. One is natural shedding, and the other is caused by the interaction of vortices with the downstream plate. The latter is the resonant vortex shedding.

4. Altering the gap distance affects the flow regime developed in the gap between the plates. At  $G = 2$ , a trapped vortex regime is established in which vortices cover the whole gap and are confined within it. At low flow velocities, the vortex is caused by natural shedding while at higher velocities, it is caused by the interaction of vortex with the edges of the plates. At  $G > 2$ , vortices that shed from the trailing edge of the upstream plate are free to move through the gap between the plates.

The above conclusions clearly identifies the flow-mechanisms responsible for the generation of lower-velocity and higher-velocity resonances in flows around tandem flat plates. This identification would help in settings tools for the prediction of resonance velocities and this is mainly important for avoiding aeroacoustic resonance in the design phase of real applications.

## REFERENCES

- Assoum, H. H., El Hassan, M., Abed-Meraim, K., & Sakout, A. (2014). The vortex dynamics and the self sustained tones in a plane jet impinging on a slotted plate. *European Journal of Mechanics - B/Fluids*, 48, 231–235. <https://doi.org/10.1016/J.EUROMECHFLU.2014.06.008>
- Assoum, H. H., Hassan, M. El, Abed-Meraïm, K., Martinuzzi, R., & Sakout, A. (2013). Experimental analysis of the aero-acoustic coupling in a plane impinging jet on a slotted plate. *Fluid Dynamics Research*, 45(4), 045503. <https://doi.org/10.1088/0169-5983/45/4/045503>
- Belvins, R. D. (1990). *Flow-Induced Vibrations* (2nd ed.). Von Nostrand Reinhold.
- Blazewicz, A. M., Bull, M. K., & Kelso, R. M. (2007). Characteristics of flow regimes for single plates of rectangular cross-section. *Proceedings of the 16th Australasian Fluid Mechanics Conference, 16AFMC, December*, 935–938.
- Bull, M. K., Blazewicz, A. M., & Pickles, J. M. (1997). Acoustic Radiation From a Tandem Two-Plate Array in a Fluid Flow: Dependence on Array Geometry and Flow Regime. *Fifth International Congress on Sound and Vibration*. [https://www.acoustics.asn.au/conference\\_proceedings/ICSVS-1997/pdf/scan/sv970425.pdf](https://www.acoustics.asn.au/conference_proceedings/ICSVS-1997/pdf/scan/sv970425.pdf)
- Di Bari, L., Ripoli, S., & Salvadori, P. (2004). Serum Albumin and Natural Products. *Progress in Biological Chirality*, 92, 271–295. <https://doi.org/10.1016/B978-008044396-6/50025-3>
- Eisinger, F. L., & Sullivan, R. E. (2007). Acoustic resonance in a package boiler and its solution- A case study. *Journal of Pressure Vessel Technology, Transactions of the ASME*, 129(4), 759–762. <https://doi.org/10.1115/1.2767369>
- El Khatib, A., Miaari, A. Al, & Hammoud, A. (2021). Aero-acoustic response of flat plates at subsonic flow. *Physica Scripta*, 96(4), 045005. <https://doi.org/10.1088/1402-4896/abd85>
- Havel, B., Hangan, H., & Martinuzzi, R. (2001). Buffeting for 2D and 3D sharp-edged bluff bodies. *Journal of Wind Engineering and Industrial Aerodynamics*, 89(14–15), 1369–1381. [https://doi.org/10.1016/S0167-6105\(01\)00152-0](https://doi.org/10.1016/S0167-6105(01)00152-0)
- Katasonov, M. M., Sung, H. J., & Bardakhanov, S. P. (2015). Wake flow-induced acoustic resonance around a long flat plate in a duct. *Journal of Engineering Thermophysics*, 24(1), 36–56. <https://doi.org/10.1134/S1810232815010051>
- Lighthill, M. (1952). On sound generated aerodynamically I. General theory. *Proceedings of the Royal Society of London. Series A. Mathematical and Physical Sciences*, 211(1107), 564–587. <https://doi.org/10.1098/rspa.1952.0060>
- Mathias, M., Stokes, A. N., Hourigan, K., & Welsh, M. C. (1988). Low-level flow-induced acoustic resonances in ducts. *Fluid Dynamics Research*, 3(1–4), 353–356. [https://doi.org/10.1016/0169-5983\(88\)90091-3](https://doi.org/10.1016/0169-5983(88)90091-3)
- Mohany, A., & Ziada, S. (2005). Flow-excited acoustic resonance of two tandem cylinders in cross-flow. *Journal of Fluids and Structures*, 21(1 SPEC. ISS.), 103–119. <https://doi.org/10.1016/j.jfluidstructs.2005.05.018>
- Mohany, A., & Ziada, S. (2009a). A parametric study of the resonance mechanism of two tandem cylinders in cross-flow. *Journal of Pressure Vessel Technology, Transactions of the ASME*, 131(2), 1–9. <https://doi.org/10.1115/1.3027452>
- Mohany, A., & Ziada, S. (2009b). Numerical simulation of the flow-sound interaction mechanisms of a single and two-tandem cylinders in cross-flow. *Journal of Pressure Vessel Technology, Transactions of the ASME*, 131(3), 1–11. <https://doi.org/10.1115/1.3110029>
- Nakamura, Y., & Hirata, K. (1989). Critical geometry of oscillating bluff bodies. *Journal of Fluid Mechanics*, 208(EM6), 375–393. <https://doi.org/10.1017/S0022112089002879>

- Parker, R. (1967). Resonance effects in wake shedding from parallel plates: Calculation of resonant frequencies. *Journal of Sound and Vibration*, 5(2), 330–343. [https://doi.org/10.1016/0022-460X\(67\)90113-7](https://doi.org/10.1016/0022-460X(67)90113-7)
- Parker, R., Hammoud, A. H., & Stoneman, S. A. T. (1993). Vortex shedding from flat plates under the influence of an acoustic field. *Journal of Wind Engineering and Industrial Aerodynamics*, 50(C), 129–138. [https://doi.org/10.1016/0167-6105\(93\)90068-Y](https://doi.org/10.1016/0167-6105(93)90068-Y)
- Parker, R., & Welsh, M. C. (1983). Effects of sound on flow separation from blunt flat plates. *International Journal of Heat and Fluid Flow*, 4(2), 113–127. [https://doi.org/10.1016/0142-727X\(83\)90014-0](https://doi.org/10.1016/0142-727X(83)90014-0)
- Sakamoto, H., Haniu, H., & Obata, Y. (1987). Fluctuating Forces Acting On Two Square Prisms in a Tandem Arrangement. *Journal of Wind Engineering and Industr*, 26, 85–103.
- Semenov, A. B., & Bardakhanov, S. P. (2007). Influence of the trailing-edge shape of a bluff body on the main resonant-regime characteristics. *Thermophysics and Aeromechanics*, 14(3), 359–362. <https://doi.org/10.1134/S0869864307030055>
- Spalart, P. R., & Allmaras, S. R. (1994). One-equation turbulence model for aerodynamic flows. *Recherche Aerospaciale*, 1, 5–21. <https://doi.org/10.2514/6.1992-439>
- Stokes, A. N., & Welsh, M. C. (1986). Flow-resonant sound interaction in a duct containing a plate, II: Square leading edge. *Journal of Sound and Vibration*, 104(1), 55–73. [https://doi.org/10.1016/S0022-460X\(86\)80131-6](https://doi.org/10.1016/S0022-460X(86)80131-6)
- Stoneman, S. A. T., Welsh, M. C., & Stokes, A. N. (1988). Resonant sound caused by flow past two plates in tandem in a duct. *Journal of Fluid Mechanics*, 192, 455–484. <https://doi.org/10.1017/S0022112088001946>
- Tan, B. T., Thompson, M. C., & Hourigan, K. (2003). Sources of acoustic resonance generated by flow around a long rectangular plate in a duct. *Journal of Fluids and Structures*, 18(6), 729–740. <https://doi.org/10.1016/j.jfluidstructs.2003.08.016>
- Welsh, M. C., & Stokes, A. N. (1984). Flow-resonant sound interaction in a duct containing a plate, I: Semi-Circular leading edge. *Journal of Sound and Vibration*, 95(3), 305–323. [https://doi.org/10.1016/S0022-460X\(86\)80131-6](https://doi.org/10.1016/S0022-460X(86)80131-6)